Study of the interaction between wind power plants and SMES systems

Federico Milano
UCD School of Electrical, Electronic and Communication Engineering
University College Dublin
Belfield, Dublin 4, Ireland
e-mail: federico.milano@ucd.ie

Rafael Zárate-Miñano
Escuela de Ingeniería de Minas e Industriales de Almadén
Universidad de Castilla - La Mancha
Almadén, Spain
e-mail: rafael.zarate@uclm.es

***Abstract*—This paper analyses the ability of a superconducting magnetic energy storage (SMES) system to reduce power fluctuations coming from the output of a wind power plant. Two control blocks are proposed to improve the transient behavior of the duty-cycle control of the SMES system. These additional blocks are aimed to reduce the number of charge/discharge processes of the SMES and to soften the abrupt transient that appears when the storage device runs out of energy. The performance of the proposed controllers is illustrated throughout simulations.**

Keywords - superconducting magnetic energy storage (SMES); transient analysis; wind fluctuations.

I. Introduction

Energy storage is considered an effective mean to improve the competitiveness of electric power production systems based on non-dispatchable generators, such as those based on renewable energy resources. The intrinsic volatility of such energy resources has a negative impact on the quality of the electrical energy supply, and complicates efficient operation. This issue can be smoothed through energy storage systems.

Several energy storage technologies are currently being developed, e.g., Compressed Air Energy Storage (CAES), Battery Energy Storage System (BESS), Superconducting Magnetic Energy Storage (SMES), Phase-Change Materials (PCM), and Flywheel Energy System (FES). The time response of energy storage systems depends on the physical principle on which they are based. For instance, the speed to store or deliver energy of a CAES system, that is driven by the mechanical dynamics of a turbine and a compressor, is typically much slower than a SMES system, which is based on electromagnetic phenomena. Time response is a key feature when it comes to select an energy storage system for a particular application.

This work discusses the use of SMES systems to reduce the power output fluctuations of wind power plants. These fluctuations are caused by wind speed variations, which are affected by ramps, gusts and stochastic disturbances. The delivery of a more constant power to the grid has two main advantages: (i) improves the quality of the power supply, and (ii) facilitates the design of bidding strategies and reduces risks in electricity markets.

The ability of SMES systems to minimize the power output fluctuations of wind power plants has already been studied in the literature. For example, [1] discusses the performance of a SMES system coupled to a wind power plant consisting of constant speed wind generators. A similar configuration is studied in [2], where some conclusions about the SMES system capacity are drawn. In [3], the authors analyze the behavior of a SMES system connected to an isolated power system. The controllers governing the SMES system are designed to dump power and voltage fluctuations coming from a wind power plant and photo-voltaic power generators in order to stabilize both the frequency and bus voltages of the power system. An extension of this study is carried out in [4], where the response of two different SMES system configurations, namely single- and double-magnet SMES systems, are presented.

With respect to ac/dc interface and the corresponding controllers, three different configurations have been proposed for SMES systems, namely thyristor-based SMES (e.g. [5]), VSC-based SMES (e.g. [1]), and CSC-based SMES (e.g. [6]). A comparison among these configurations in terms of real and reactive power control abilities, control structure, harmonic distortion level, and SMES coil voltage ripple is provided in [7]. Finally, [7] provides an overview of SMES applications in power systems, whereas an extensive literature review of energy storage systems for wind power applications can be found in [8].

The focus of this work is on the dynamic interaction between a wind power plant and a SMES system. A SMES system model is proposed, including the control blocks needed to govern its performance. The proposed model is tested throughout simulations.

II. SMES Model

Figure 1 depicts a SMES device coupled to a wind power plant. The objective of the SMES device is to smooth the fluctuations in the power output of the wind power plant such that the power flow through the transmission line, that connects the wind power plant to the power system, follows a given reference value. The SMES device consists of the following basic components: (i) Voltage Source Converter (VSC); (ii) boost converter; and (iii) superconducting coil.

Figure 2 shows the VSC scheme. The usual configuration includes a transformer, a by-directional inverter, and a con-

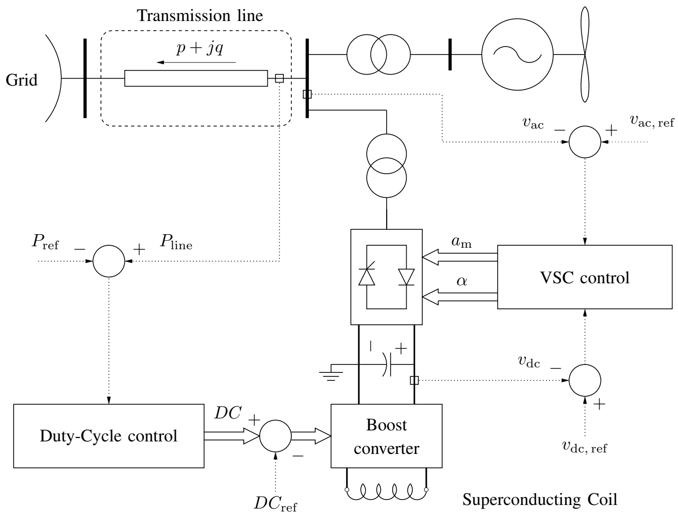

Fig. 1. Scheme of a SMES system coupled to a wind power plant

denser. The transformer provides galvanic isolation, whereas the condenser maintains the voltage level at the dc side of the converter. The dc voltage is transformed to ac voltage by a proper control logic of the static switches. The variables involved in this control logic are the modulation amplitude $a_{\rm m}$, and the firing angle α.

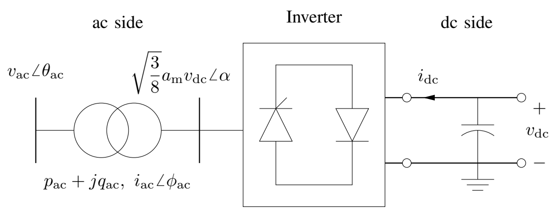

Fig. 2. Scheme of a Voltage Source Converter

The equations of the ac side of the inverter are as follows:

$$p_{\rm ac} = g_{\rm t} v_{\rm ac}^2 - \kappa g_{\rm t} \cos(\theta_{\rm ac} - \alpha) - \kappa b_{\rm t} \sin(\theta_{\rm ac} - \alpha) \quad (1)$$
$$q_{\rm ac} = -b_{\rm t} v_{\rm ac}^2 + \kappa b_{\rm t} \cos(\theta_{\rm ac} - \alpha) - \kappa g_{\rm t} \sin(\theta_{\rm ac} - \alpha)$$

where $\kappa = \sqrt{\frac{3}{8}} a_{\rm m} v_{\rm dc} v_{\rm ac}$ and $g_{\rm t} + jb_{\rm t} = 1/(r_{\rm t} + jx_{\rm t})$ is the series admittance of the transformer. The power balance between the dc and the ac sides of the inverter is imposed by

$$0 = g_{\rm t} \frac{3}{8} a_{\rm m}^2 v_{\rm dc}^2 - \kappa g_{\rm t} \cos(\theta_{\rm ac} - \alpha) - \kappa b_{\rm t} \sin(\theta_{\rm ac} - \alpha) \quad (2)$$

The VSC performance is controlled through two blocks, indicated in Figure 1 as the VSC control. The first block controls the voltage magnitude at the ac side of the SMES. The VSC control takes the difference between the ac voltage amplitude and the reference voltage (i.e., $v_{\rm ac,\,ref} - v_{\rm ac}$) as the input signal, and modifies the modulation amplitude $a_{\rm m}$ of the VSC accordingly. This block is designed as a lead/lag controller, whose input signal is previously filtered by means of a low-pass filter, as depicted in Figure 3.

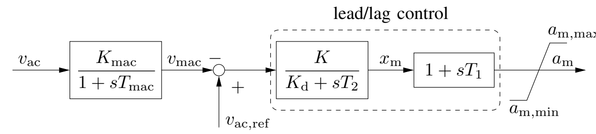

Fig. 3. Modulation amplitude controller of the VSC

The other control block of the VSC regulates the voltage at the dc side of the SMES. This block takes the deviation of the dc voltage from the reference (i.e., $v_{\rm dc,\,ref} - v_{\rm dc}$) as the input signal, and accordingly modifies the firing angle α of the VSC components. This control block is designed as a proportional-integral (PI) controller, whose input signal is previously filtered by means of a low-pass filter, as depicted in Figure 4.

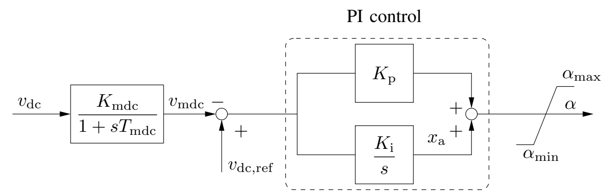

Fig. 4. Firing angle controller of the VSC

The superconducting coil is connected in parallel to the VSC throughout a dc/dc converter (boost converter). Figure 5 depicts the connection scheme of the boost converter and the superconducting coil. The superconducting coil stores

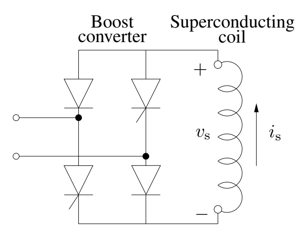

Fig. 5. Connection of the boost converter and the superconducting coil

magnetic energy and injects it into the network depending on the duty cycle of the boost converter. The performance of the set consisting of boost converter and superconducting coil is modelled by the following equations:

$$\frac{di_{\rm s}}{dt} = -\frac{v_{\rm s}}{L} \quad (3)$$
$$v_{\rm s} = (1 - 2DC)\, v_{\rm dc} \quad (4)$$
$$i_{\rm dc} = (1 - 2DC)\, i_{\rm s} \quad (5)$$

where all currents and voltages are mean values, L is the inductance of the superconducting coil, and DC is the duty cycle of the boost converter. The expression of the energy stored in the superconducting coil is as follows:

$$E = \frac{1}{2} L i_{\rm s}^2 \quad (6)$$

The charging/discharging process of the superconducting coil is controlled by the duty-cycle control (see Figure 1). The input signal is the error between the actual active power flow through the transmission line and the active power reference (i.e., $P_{\text{line}} - P_{\text{ref}}$). If the power flowing in the transmission line deviates from the reference, a duty cycle signal DC is delivered to the boost converter. This converter governs the charging/discharging process of the superconducting coil. In this work, the main block of the duty-cycle control is designed as a PID controller, whose input signal is previously filtered by means of a low-pass filter, as depicted in Figure 6.

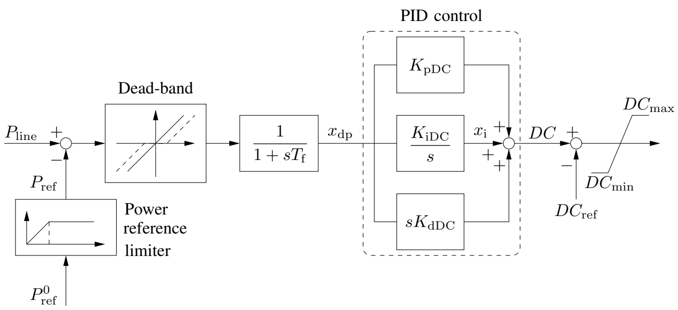

Fig. 6. Duty-cycle control of the superconducting coil

If $P_{\text{line}} = P_{\text{ref}}$, the superconducting coil remains short-circuited. In steady-state, this situation corresponds to $DC = DC_{\text{ref}}$ (typically, $DC_{\text{ref}} = 0.5$). Any deviation of P_{line} from P_{ref} will imply $DC \neq DC_{\text{ref}}$, and the superconducting coil will inject current to the ac bus through the VSC (discharge process) or absorb current from the ac bus (charge process), respectively.

This work proposes two additional blocks to improve the transient behavior of the duty-cycle control: a dead-band block, and a power reference limiter (see Figure 6). The dead-band block is designed to reduce the sensitivity of the duty-cycle control to small changes in the deviation of the controlled power flow with respect to the reference. The dead-band block reduces the number of charge/discharge processes of the SMES and, thus, increases the life of the device. The power reference limiter is included to smooth transients that can occur if the SMES runs out of energy. The main purpose of this block is to avoid abrupt steps in the power production of the joint system formed by the wind turbine and the SMES device. The reference power is activated by the value of the energy stored in the SMES, as follows:

$$P_{\text{ref}} = \begin{cases} \dfrac{E}{E_{\text{thr}}} P^0_{\text{ref}} & \text{if } E < E_{\text{thr}} \\ P^0_{\text{ref}} & \text{otherwise.} \end{cases} \tag{7}$$

The effect of the dead-band and the reference power limiter on the response of the SMES device as well as of the overall system is illustrated in the following section.

III. Simulations

The proposed control system is tested by using the power system configuration shown in Figure 1. This power system consists of a SMES device coupled to a wind power plant whose output power is injected to a transmission network. The wind power plant is modelled as an equivalent single wind generator of the DFIG type [9]. The SMES device and the proposed controllers are modelled as described in the previous section. All models has been implemented in DOME [10], which is a Python- and C-based next-generation version of PSAT [11].

As an example of the performance of the proposed control system, Figure 7 compares the power flow through the transmission line when the wind power plant is working with and without the SMES system. In both cases, the wind power plant undergoes a standard wind perturbation of the Mexican-hat type. It can be observed that, without the SMES device, the power injected into the grid necessarily follows the wind perturbation. However, if the SMES device is coupled to the wind power plant, the power flow through the transmission line remains almost constant.

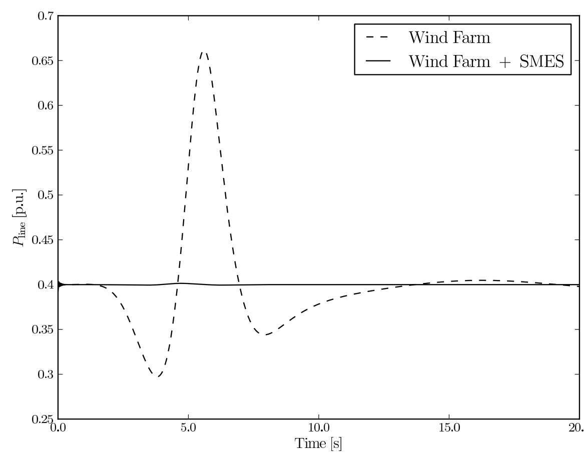

Fig. 7. Power flow through the transmission line with and without the SMES system

Figure 8 shows the effect of the power reference limiter. The system and the perturbation are the same as that shown in Figure 7, except for the initial energy stored in the SMES, which is the half of the one used in the previous simulation. In this case, if the reference power is maintained constant, the SMES runs out of energy and cannot fully control the active power in the transmission line. As a consequence, the power injected into the grid suffers a drop of about 25%. As it can be observed from Figure 8, relaxing the control on the active power by introducing an energy threshold of 5% allows to avoid fully consuming the energy stored in the SMES and, thus, consistently reduces the drop of the power injected into the grid.

Finally, Figure 9 shows the response of the system composed of the equivalent wind turbine and the SMES device for a wind speed that follows a Weibull distribution. If no dead-band is enforced, the superconducting coil is continuously charged and

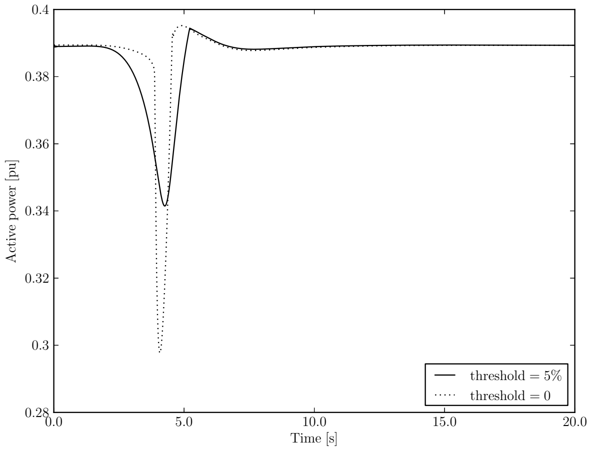

Fig. 8. Power flow through the transmission line with SMES for different values of the energy threshold of the reference power limiter

discharged. The dead-band can drastically reduce the number of charge and discharge operations at the cost of a deviation with respect to the reference active power. The amount of such deviation depends on the size of the dead-band.

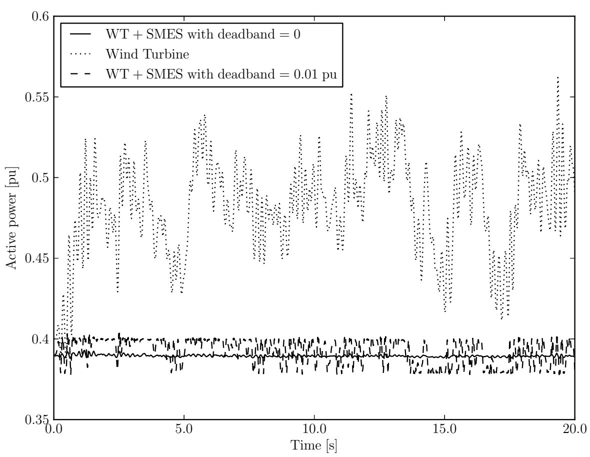

Fig. 9. Power flow through the transmission line with SMES with and without enforcing the dead-band over the power control

IV. Conclusions

This paper discusses some aspects of the dynamic performance of a SMES system coupled to a wind power plant. This configuration is aimed at reducing active power fluctuations of wind generators. A set of controllers for the SMES system, including a dead-band block and a power reference limiter, is proposed and tested throughout simulations. Results show that the proposed controllers are able to improve the dynamic response of the SMES system. The dead-band block reduces the sensitivity of the duty cycle control to small changes in the deviation of the controlled power flow with respect to the reference. In this way, the life of the SMES is increased since the number of charge/discharge processes of the device is reduced. On the other hand, the power reference limiter avoids abrupt transients when the SMES system runs out of energy.

References

[1] F. Zhou, G. Joos, C. Abbey, L. Jiao, and B. T. Ooi, "Use of large capacity SMES to improve the power quality and stability of wind farms," in *IEEE PES General Meeting*, vol. 2, Denver, CO, USA, Jun. 2004, pp. 2025–2030.

[2] T. Asao, R. Takahashi, T. Murata, J. Tamura, M. Kubo, A. Kuwayama, and T. Matsumoto, "Smoothing control of wind power generator output by superconducting magnetic energy storage system," in *Int. Conf. Electrical Machines and Systems 2007 (ICEMS 2007)*, Seoul, South Korea, Oct. 2007, pp. 302–307.

[3] H. Y. Jung, A. R. Kim, J. H. Kim, M. Park, I. K. Yu, S. H. Kim, K. Sim, H. J. Kim, K. C. Seong, T. Asao, and J. Tamura, "A study on the operating characteristics of SMES for the dispersed power generation system," *IEEE Transactions on Applied Superconductivity*, vol. 19, no. 3, pp. 2028–2031, Jun. 2009.

[4] A. R. Kim, H. R. Seo, G. H. Kim, M. Park, I. K. Yu, Y. Otsuki, J. Tamura, S. H. Kim, K. Sim, and K. C. Seong, "Operating characteristic analysis of HTS SMES for frequency stabilization of dispersed power generation system," *IEEE Transactions on Applied Superconductivity*, vol. 20, no. 3, pp. 1330–1334, Jun. 2010.

[5] J. B. X. Devotta and M. G. Rabbani, "Application of superconducting magnetic energy storage unit in multi-machine power systems," *Energy Conversion and Management*, vol. 41, no. 5, pp. 493–504, Mar. 2000.

[6] K. Imaie, O. Tsukamoto, and Y. Nagai, "Control strategies for multiple parallel current-source converters of SMES system," *IEEE Transactions on Power Electronics*, vol. 15, no. 2, pp. 377–385, Mar. 2000.

[7] M. H. Ali, B. Wu, and R. A. Dougal, "An overview of SMES applications in power and energy systems," *IEEE Transactions on Sustainable Energy*, vol. 1, no. 1, pp. 38–47, Apr. 2010.

[8] F. Díaz-González, A. Sumper, O. Gomis-Bellmunt, and R. Villafáfila-Robles, "A review of energy storage technologies for wind power applications," *Revewable and Sustainable Energy Reviews*, vol. 16, no. 4, pp. 2154–2171, May 2012.

[9] F. Milano, *Power System Modelling and Scripting*. London: Springer, 2010.

[10] ——, "Dome Program," 2013, University College Dublin, available at faraday1.ucd.es/dome.html.

[11] ——, "An open source power system analysis toolbox," *IEEE Transactions on Power Systems*, vol. 20, no. 3, pp. 1199–1206, Aug. 2005.